Geospatial Modeling of Soil Erosion and Conservation Priorities: A Case Study from the Panam Reservoir, India

Amanullah Hayat* and T.M.V. Suryanarayana

Water Resources Engineering and Management Institute, Faculty of Technology and Engineering, The Maharaja Sayajirao University of Baroda, Vadodara 390 002, India

Received: February 21, 2025 Accepted: March 18, 2025

Abstract: Soil erosion presents a significant threat to the sustainability of land and water resources in the Panam Reservoir region of Gujarat, India. This study utilizes the Revised Universal Soil Loss Equation (RUSLE), integrated with advanced geospatial techniques, to quantify soil loss and identify erosion-prone areas. Spatial datasets on rainfall erosivity, soil erodibility, topography, land use, and conservation practices were analyzed using Geographic Information Systems (GIS) and remote sensing tools. The results indicate that annual soil loss ranges from zero to 28.226 t ha⁻¹ yr⁻¹, with most of the catchment experiencing low erosion risk. However, a smaller portion of the area is subjected to moderate to severe erosion, highlighting the need for targeted conservation interventions. Vulnerable zones are characterized by steep slopes, high rainfall erosivity, and sparse vegetation cover. This research provides spatially explicit insights crucial for informed soil conservation planning and watershed management in similar agroecological contexts. The integration of RUSLE with remote sensing and GIS enhances the precision of erosion assessment, thereby supporting sustainable land use decision-making.

Key words: Soil erosion, RUSLE, GIS, remote sensing, Panam reservoir, conservation planning.

Soil erosion is a significant environmental issue affecting agricultural productivity, reservoir capacity, and ecosystem stability. Globally, erosion reduces the fertility of arable lands and accelerates sedimentation in water bodies. In India, an estimated 5.3 billion tons of soil are lost annually, affecting more than 145 million hectares (NAAS, 2010). The Panam Reservoir, located in the Mahi River basin in Gujarat, plays a vital role in regional water supply and irrigation. The reservoir's catchment features varied topography, diverse soil types (loam and clay), and intense monsoonal rainfall, all contributing to erosion risk. Accurate assessment of soil erosion is crucial for effective management of this water resource. This study addresses the need for a spatially detailed evaluation of erosion risk using the RUSLE model in a GIS environment. It aims to support conservation efforts by identifying vulnerable zones and quantifying soil loss across the catchment.

OPEN ACCESS

Editor-in-Chief
Praveen Kumar

Editors (India)

Anita Pandey Hema Yadav Neena Singla Ritu Mawar Sanjana Reddy Surendra Poonia R.K. Solanki P.S. Khapte

Editors (International)

M. Faci, Algeria M. Janmohammadi, Iran

*Correspondence

Amanullah Hayat hayatamanullah945@gmail.com

Citation

Hayat, A. and Suryanarayana, T.M.V. 2025. Geospatial modeling of soil erosion and conservation priorities: A case study from the Panam reservoir, India. Annals of Arid Zone 64(2): 289-298

> https://doi.org/10.56093/aaz. v64i2.165215

https://epubs.icar.org.in/index.php/AAZ/ article/view/165215

Materials and Methods

Study area: The Panam Reservoir is situated in Santrampur Taluka of Mahi Sagar district, Gujarat, India. Geographical boundaries of the area are given in Fig 1. The catchment area spans 2363.87 km². The region is characterized by undulating terrain, slopes ranging from 0-50%, and soils dominated by loam upstream and clay downstream. Annual rainfall varies significantly, with erosion primarily driven by intense monsoonal storms.

Data Sources: Topographic map of the area, data on soil properties, rainfall, satellite and others were collected from authorized sources viz. topographic maps: survey of India (1:50,000 scale), soil data: FAO and UNESCO soil database, rainfall data: India Meteorological Department (1994-2023), Satellite imagery: Landsat 5, 7, and 8 (1994-2023).: ArcGIS 10.7.1, Erdas Imagine 2014 and, MS Excel were the main tools to process the data. To quantify spatial and temporal patterns of soil erosion within the Panam catchment, the Revised Universal Soil Loss Equation (RUSLE) was applied within a GIS environment. This empirical model estimates the annual average soil loss per unit area (t ha-1 yr-1) by integrating five key biophysical factors:

where, A = average annual soil loss (t ha⁻¹ yr⁻¹), R = rainfall erosivity factor, K = soil erodibility factor, LS = slope length and steepness factor, C = cover management factor, and P = support practice factor.

...1

Instead of using general global coefficients, rainfall erosivity was estimated using a regionally calibrated equation based on long-term rainfall data from the India Meteorological Department (IMD), following the approach by Ghosal and Maiti (2021). This captures the kinetic energy and intensity of monsoonal storms typical to Gujarat, which have a significant influence on surface runoff and subsequent detachment of soil particles.

$$R = 79 + 0.363 \times P$$
 ...2

where, P is annual precipitation in mm. Resulting, R-values ranged from 280.75 to 592.12 MJ mm ha⁻¹ hr⁻¹ yr⁻¹. The following table 1 indicates R-Factor values from 1994 to 2023

K-values were calculated based on FAO soil texture datasets and field-verified information on clay and loam soils within the basin. The erodibility estimates factored in local texture proportions, organic matter content (derived from soil carbon), structure

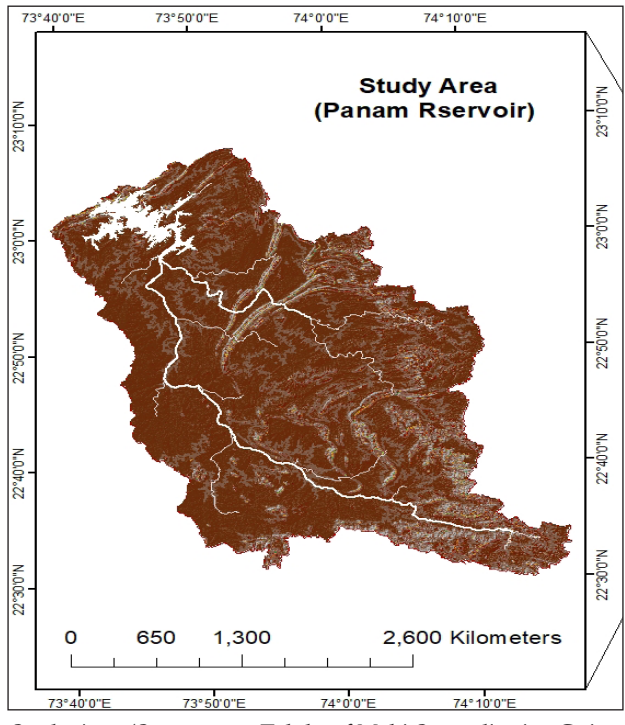


Fig. 1. Study Area (Santrampur Taluka of Mahi Sagar district, Gujarat, India).

Table 1. Rainfall erosivity (R) values

Year(s)	Annual-Average rainfall (mm)	R-factor (MJ mm ha-hr ⁻¹ yr ⁻¹)
1994	1392.24	584.36
1999	555.650	280.75
2004	948.970	423.45
2009	599.490	296.61
2014	764.740	356.60
2015	594.240	294.70
2016	788.490	365.22
2017	844.510	385.56
2018	716.270	339.01
2019	1413.57	592.12
2020	919.340	412.72
2021	723.760	341.72
2022	818.500	376.11
2023	987.850	437.59

Average annual R factor is = 377.645 to 427.009

type, and permeability class. Loamy areas in the southeastern catchment showed higher susceptibility (K \approx 0.164), whereas clayey zones displayed comparatively lower values (K \approx 0.101) due to their cohesive properties (Wischmeier and Smith, 1978):

$$K=[(2.1 \times 10^{-4} \times M^{1.14} \times (12-OM)+3.25 \times (Structure-2)+2.5 \times Permeability-3)]/100$$
 ...3

where, M = (%silt + % very fine sand)*(100 - % clay); very fine sand= 7% for clay and 15% for loam; OM = organic carbon * 1.72; Structure = soil structure considered 3 for clay/loam; permeability = permeability considered 2 for clay, 4 for loam.

Calculated K-values ranged from 0.101 for clay-rich zones to 0.164 for loamy regions (Table 2). These estimates were adapted for local conditions using assumed inputs consistent with FAO-derived soil properties and verified against erosion literature from western India. Table 2 also presents the key soil properties and corresponding K-factor values (soil erodibility) used in the RUSLE model for the Panam catchment. Two dominant

soil types were identified: clay and loam. The K-factor, which quantifies the susceptibility of soil to erosion by rainfall and surface runoff, was calculated using the Wischmeier and Smith (1978) empirical equation, incorporating inputs such as soil texture (clay, silt, very fine sand), organic matter content, structure, and permeability class.

The results (Table 2) further show that clay soils exhibit a lower K-factor (0.101) due to their cohesive properties and slower permeability but Loam soils have a higher K-factor (0.164), indicating greater vulnerability to detachment under rainfall impact. These calibrated K-values were mapped spatially (see K-factor map) and integrated into the RUSLE model to reflect localized soil behaviour in erosion estimation. The table justifies the differentiation in soil erodibility across the basin, which is critical for understanding spatial variations in erosion risk and for designing targeted soil conservation strategies.

Topographic Factor (LS): Derived from the Copernicus 30 m DEM, the LS factor was calculated using the Moore and Burch method within ArcGIS hydrology tools. The relief-tolength (R/L) ratio was also computed for SDR modelling. The LS-Factor has been calculated by equation 4, Singh, S.K. *et al.* (2017), Moore, I.D. and Burch, G.J. (1986).

$$LS = 0.0138 \times (S^{0.39}) \times (L^{0.33}) \times (\theta^{0.14}) \qquad ...4$$

where, LS = Topographic factor (dimensionless); S = Slope steepness (slope %); L = Slope length (meters); θ = Slope angle (degrees)

For the current study LS factor varies from 0 to 3.29 with the mean value of 0.025, with a standard deviation of 0.065. The steep terrains, particularly in the upper basin and areas marked in red, exhibit higher LS-factor values compared to the flatter terrain in the middle and lower watershed areas. LS-factor values range from 2-2.8 and 2.8-3.29 in the upper catchment and parts of the middle area, while the lower catchment displays lower values, ranging from

Table 2. Soil Properties and Calculated K-Factor in the Panam Catchment

Soil type	Texture class	% clay	% silt	% Very fine sand	Organic carbon (%)	Organic matter (%)	Structure code	Permeability code	K-Factor
Clay	Fine- textured	40	25	7	0.9	1.55	3	2	0.101
Loam	Medium- textured	18	38	15	0.8	1.38	3	4	0.164

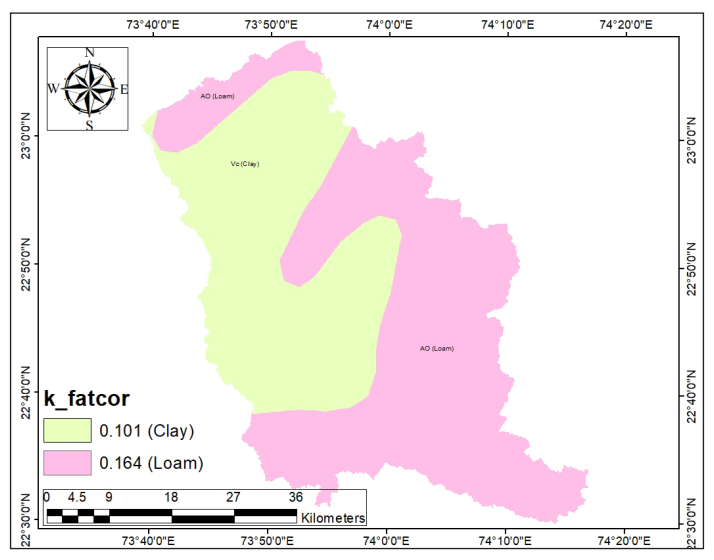


Fig. 2. Soil Erodibility K-factor.

0.5-1.2, and 1.2-2, In general, the LS-factor is directly proportional to the susceptibility of an area to erosion, with higher LS-factor values indicating more erosion-prone regions

Cover management factor (C): Vegetation influence on erosion was captured through Normalized Difference Vegetation Index (NDVI) derived from Landsat imagery for each selected year. The NDVI was converted to C-values using the equation developed by Van der Knijff et al. (2000), also used at continental scales by (Panagos et al., 2015). allowing dynamic tracking of how seasonal and annual vegetation fluctuations influenced soil protection. Higher C-values were recorded in bare or agricultural lands, whereas densely

vegetated zones showed significantly reduced erosion potential.

$$C = 0.4231 \times e^{-0.2403*NDVI}$$
 ...5
 $C = a \times e^{-b*NDVI}$...6
 $NDVI = (NIR-R)/(NIR+R)$...7

where C = C-Factor (dependent variable); NDVI = Normalized Difference Vegetation Index (independent variable); a and b = Regression coefficients to be determined; e = Euler's number (constant) (≈ 2.7183).

In order to calculate the coefficients a, and b the regression has been applied and the result was equation 5 based on which I have calculate c factor.

$$C = 0.4231 \text{ x e}^{-0.2403*\text{NDVI}}$$
 ...5

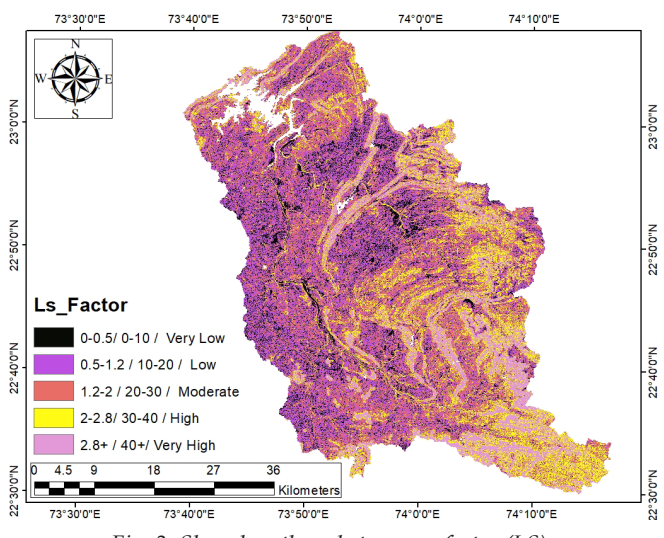


Fig. 3. Slope-length and steepness factor (LS).

Table 3. NDVI and C-factor's Values

	,	
Years	NDVI (mean)	C_Factor (mean)
1994	0.112723676	0.411794265
1999	0.069850574	0.416058221
2009	0.179057154	0.405282999
2014	0.187701244	0.404442116
2015	0.166353712	0.406521942
2016	0.178524177	0.405334903
2017	0.181535026	0.405041777
2018	0.186241299	0.404584014
2019	0.200437967	0.403206287
2020	0.197420469	0.403498729
2021	0.198551292	0.403389111
2022	0.304962741	0.393205985
2023	0.212285033	0.402060171

The following table summarizes how NDVI ranges were translated into cover factors for various land types in the study area.

These values were derived using NDVI ranges obtained from multi-year Landsat imagery and processed according to the exponential model developed by Van der Knijff *et al.* (2000). The C-Factor quantifies the effect of vegetation cover on soil erosion, where lower values indicate better protection against erosion. For instance: Dense vegetation and water bodies exhibit very low C-factors (close to 0), reflecting minimal erosion potential. Crop and agricultural lands, which experience seasonal vegetation changes, show moderate C-factors. Bare land and built-up areas are assigned higher C-values due to their lack of protective cover, indicating high susceptibility to erosion.

These class-based C-Factor values were used to generate spatially distributed C-factor rasters for each analysis year, which were then integrated into the RUSLE model to assess erosion dynamics across the basin.

Support Practice Factor (P): The P-factor, which reflects the effectiveness of soil conservation structures, was indirectly estimated using slope-based proxies and NDVI-derived land condition indicators. The empirical model proposed by Prasannakumar *et al.* (2012), was adopted, offering a context-appropriate method to assign spatially variable P-values across the basin. This approach accounts for the lack of direct data on conservation structures while still representing realistic management effects.

All five RUSLE factors were prepared as raster layers with a 30-meter resolution and integrated spatially in ArcGIS 10.8 to generate annual erosion estimates from 1994 to 2023. The resulting maps provide a high-resolution visualization of soil erosion intensity across the Panam watershed, supporting both temporal trend analysis and hotspot identification.

$$P = 0.429 - 0.051 \times (NDVI) + 0.0023 \times S$$
 ...8 where, NDVI: Normalized Difference Vegetation Index; S: Slope steepness (%)

$$NDVI = (NIR-R)/(NIR+R) \qquad ...7$$

where, NIR (Near-Infrared Band) reflects strongly in healthy vegetation; R (Red Band) is absorbed by chlorophyll in plants and healthy vegetation has low R. in the Landsat 8 and 9 images, the NIR is considers as band 5 and R as band 4 while for Landsat 7, 5, 4 band 5 and band 4 replaces their positions to band 4 and 3 respectively. P factor for the current study varies from 0.4 to 0.433, and has been categorized bellow Table 5 based on the Gujarat state disaster management authority GSDMA (2017), Soil Conservation Service (SCS) and FAO (Soil Erosion Assessment, 2003) that illustrate the P-factor and it is risk to the region.

Table 6 presents the slope-based classification of the support practice factor (P-Factor), reflecting the effectiveness of land management

Table 4. Assigned C-Factor values based on land cover and NDVI ranges in the Panam catchment

Land cover class	Typical NDVI range	Assigned C-Factor	Remarks
Water Bodies	< 0.05	0.00	No erosion - permanent water
Vegetation	0.25 - 0.45	0.01 - 0.10	Dense vegetation - strong soil protection
Flooded Vegetation	0.15 - 0.30	0.10 - 0.20	Seasonal vegetation cover, temporary protection
Crop Land	0.10 - 0.25	0.20 - 0.35	Variable cover - moderate erosion risk
Agricultural Land	0.08 - 0.22	0.35 - 0.45	Sparse cover during off-season
Bare Land	0.05 - 0.15	0.50 - 0.65	High erosion risk - little to no vegetation
Built-up Area	< 0.10	0.40 - 0.50	Minimal vegetation cover

Table 5. P-factor and it's relation with slope and soil erosion risk

Slope (%)	NDVI	P-Factor	Soil Erosion Risk
6.9	0.072-0.1	0.40-0.41	Low risk
18.5	0.1-0.25	0.41-0.42	Modert risk
36.2	0.25-0.35	0.42-0.425	High risk
110.6	0.35-0.42	0.425-0.433	Very and extremely high risk

Table 6. Slope classes and assigned P-Factor in the Panam Catchment

Slope (%)	NDVI Range	Assigned P-Factor	Soil Erosion Risk Level
0-10	0.07-0.10	0.40-0.41	Low Risk
10-20	0.10-0.25	0.41-0.42	Moderate Risk
20-35	0.25-0.35	0.42-0.425	High Risk
>35	0.35-0.42	0.425-0.433	Very High to Extremely High Risk

practices in reducing erosion. The classification integrates slope gradient and NDVI values following empirical relationships adapted from GSDMA (2017), SCS (2003), and FAO (2003). Lower P-values correspond to better conservation measures (e.g. in flatter, vegetated areas), while higher values indicate increased erosion risk in steep or poorly vegetated slopes. This classification allowed for spatially variable P-factor assignment across the basin using DEM and NDVI data.

Results and Discussion

This section presents the comprehensive results of spatial and temporal soil erosion

modelling, sediment delivery, and sediment yield dynamics in the Panam Reservoir catchment from 1994 to 2023. The analysis synthesizes multi-year geospatial outputs from the RUSLE model, SDR calculations, reservoir storage data, and LULC transitions, providing insight into long-term erosion patterns and sedimentation risks.

Spatial Distribution of Soil Erosion Risk: The RUSLE-derived soil erosion maps revealed considerable spatial variability across the 2363 km² catchment, driven primarily by topography, land cover, and vegetation density. Erosion risk was categorized based on FAO (2003) thresholds i.e. low risk (<10 t ha-1 yr-1 concentrated in flat, vegetated areas and water bodies); moderate risk (10-20 t ha-1 yr-1 primarily in agricultural transition zones); high to very vigh risk (>20 t ha-1 yr-1 observed on steep bare lands, degraded croplands, and areas with low NDVI). The maximum erosion value reached 40.07 t ha⁻¹ yr⁻¹ in 2019, coinciding with reduced vegetative cover and high rainfall intensity. The mean annual soil loss over the 30-year period was calculated as 28.27 t ha⁻¹ yr⁻¹, suggesting persistent moderate to severe erosion risk across large portions of the watershed. The following figure 2 indicates Average Annual Soil Erosion Rate and Risk Zonation in Panam Reservoir Catchment

Temporal variations in soil erosion (SE) trends: Soil erosion rates fluctuated in response to interannual variability in land cover and

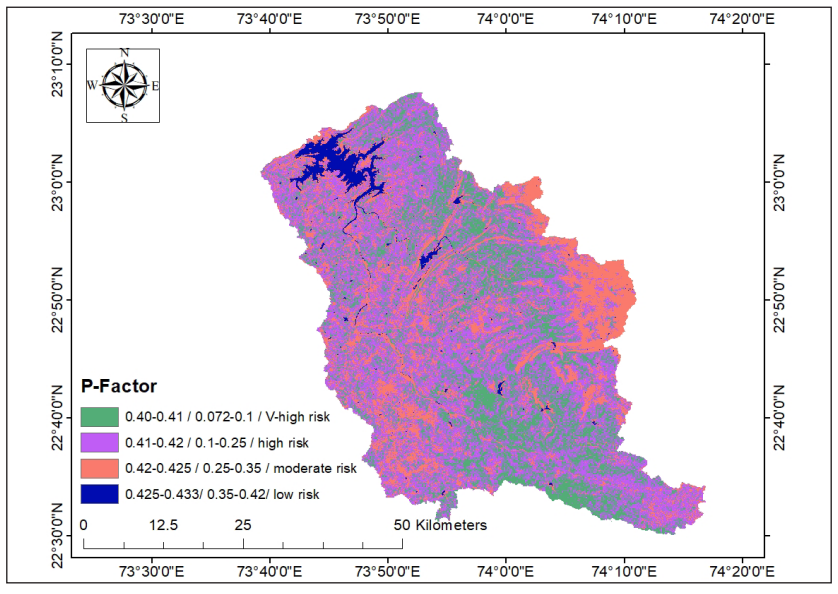


Fig. 4. Support Practice Factor (P)

Table 7. Temporal Variation of CN, Soil Erosion SE, in Panam Catchment (1994-2023)

Year (s) Area km² R/L km² CN (t ha¹¹ yr¹¹) 1994 2363 0.14382079 66.69 39.5563 1999 2363 0.14382079 78.125 20.9159 2004 2363 0.14382079 73.352 29.0002 2009 2363 0.14382079 84.488 21.4606 2014 2363 0.14382079 77.876 26.2655 2015 2363 0.14382079 77.985 26.0074 2016 2363 0.14382079 78.949 27.6847 2018 2363 0.14382079 80.511 22.4661 2019 2363 0.14382079 80.072 40.0671 2020 2363 0.14382079 79.415 30.8829 2021 2363 0.14382079 80.519 24.6555 2022 2363 0.14382079 79.642 27.9756 2023 2363 0.14382079 80.031 30.1578			(/	
1999 2363 0.14382079 78.125 20.9159 2004 2363 0.14382079 73.352 29.0002 2009 2363 0.14382079 84.488 21.4606 2014 2363 0.14382079 77.876 26.2655 2015 2363 0.14382079 84.373 21.2337 2016 2363 0.14382079 77.985 26.0074 2017 2363 0.14382079 78.949 27.6847 2018 2363 0.14382079 80.511 22.4661 2019 2363 0.14382079 80.072 40.0671 2020 2363 0.14382079 79.415 30.8829 2021 2363 0.14382079 80.519 24.6555 2022 2363 0.14382079 79.642 27.9756	Year (s)		R/L	CN	(t ha ⁻¹
2004 2363 0.14382079 73.352 29.0002 2009 2363 0.14382079 84.488 21.4606 2014 2363 0.14382079 77.876 26.2655 2015 2363 0.14382079 84.373 21.2337 2016 2363 0.14382079 77.985 26.0074 2017 2363 0.14382079 78.949 27.6847 2018 2363 0.14382079 80.511 22.4661 2019 2363 0.14382079 80.072 40.0671 2020 2363 0.14382079 79.415 30.8829 2021 2363 0.14382079 80.519 24.6555 2022 2363 0.14382079 79.642 27.9756	1994	2363	0.14382079	66.69	39.5563
2009 2363 0.14382079 84.488 21.4606 2014 2363 0.14382079 77.876 26.2655 2015 2363 0.14382079 84.373 21.2337 2016 2363 0.14382079 77.985 26.0074 2017 2363 0.14382079 78.949 27.6847 2018 2363 0.14382079 80.511 22.4661 2019 2363 0.14382079 80.072 40.0671 2020 2363 0.14382079 79.415 30.8829 2021 2363 0.14382079 80.519 24.6555 2022 2363 0.14382079 79.642 27.9756	1999	2363	0.14382079	78.125	20.9159
2014 2363 0.14382079 77.876 26.2655 2015 2363 0.14382079 84.373 21.2337 2016 2363 0.14382079 77.985 26.0074 2017 2363 0.14382079 78.949 27.6847 2018 2363 0.14382079 80.511 22.4661 2019 2363 0.14382079 80.072 40.0671 2020 2363 0.14382079 79.415 30.8829 2021 2363 0.14382079 80.519 24.6555 2022 2363 0.14382079 79.642 27.9756	2004	2363	0.14382079	73.352	29.0002
2015 2363 0.14382079 84.373 21.2337 2016 2363 0.14382079 77.985 26.0074 2017 2363 0.14382079 78.949 27.6847 2018 2363 0.14382079 80.511 22.4661 2019 2363 0.14382079 80.072 40.0671 2020 2363 0.14382079 79.415 30.8829 2021 2363 0.14382079 80.519 24.6555 2022 2363 0.14382079 79.642 27.9756	2009	2363	0.14382079	84.488	21.4606
2016 2363 0.14382079 77.985 26.0074 2017 2363 0.14382079 78.949 27.6847 2018 2363 0.14382079 80.511 22.4661 2019 2363 0.14382079 80.072 40.0671 2020 2363 0.14382079 79.415 30.8829 2021 2363 0.14382079 80.519 24.6555 2022 2363 0.14382079 79.642 27.9756	2014	2363	0.14382079	77.876	26.2655
2017 2363 0.14382079 78.949 27.6847 2018 2363 0.14382079 80.511 22.4661 2019 2363 0.14382079 80.072 40.0671 2020 2363 0.14382079 79.415 30.8829 2021 2363 0.14382079 80.519 24.6555 2022 2363 0.14382079 79.642 27.9756	2015	2363	0.14382079	84.373	21.2337
2018 2363 0.14382079 80.511 22.4661 2019 2363 0.14382079 80.072 40.0671 2020 2363 0.14382079 79.415 30.8829 2021 2363 0.14382079 80.519 24.6555 2022 2363 0.14382079 79.642 27.9756	2016	2363	0.14382079	77.985	26.0074
2019 2363 0.14382079 80.072 40.0671 2020 2363 0.14382079 79.415 30.8829 2021 2363 0.14382079 80.519 24.6555 2022 2363 0.14382079 79.642 27.9756	2017	2363	0.14382079	78.949	27.6847
2020 2363 0.14382079 79.415 30.8829 2021 2363 0.14382079 80.519 24.6555 2022 2363 0.14382079 79.642 27.9756	2018	2363	0.14382079	80.511	22.4661
2021 2363 0.14382079 80.519 24.6555 2022 2363 0.14382079 79.642 27.9756	2019	2363	0.14382079	80.072	40.0671
2022 2363 0.14382079 79.642 27.9756	2020	2363	0.14382079	79.415	30.8829
	2021	2363	0.14382079	80.519	24.6555
2023 2363 0.14382079 80.031 30.1578	2022	2363	0.14382079	79.642	27.9756
	2023	2363	0.14382079	80.031	30.1578

precipitation. Three key erosion peaks were recorded during the study period (Fig. 2). First key erosion peaks was recorded in 1994 (39.55 t ha⁻¹ yr⁻¹). which was associated with sparse vegetation and early land degradation. Another peak was recorded in 2004. It was lower than that of 1994 and was moderated by vegetation recovery. Third peak was recorded in 2019 which was very close to that of 1994. The periods between 2019 - 2023 was also the period of increased imperviousness and

cropland disturbance and as a consequence high erosion values were consistently recorded during this period. This trend also reflected the intensifying land pressure and climate volatility affecting sediment mobilization in the catchment.

The graph illustrates the temporal variation in annual average soil erosion over a 30-year period. Soil loss ranged from a low of 20.92 t ha⁻¹ yr⁻¹ in 1999 to a peak of 40.07 t ha⁻¹ yr⁻¹ in 2019. The highest erosion rates were observed in 1994 and 2019, which may be attributed to intense monsoonal rainfall events and reduced vegetation cover. Conversely, years like 1999, 2009, and 2015 recorded lower erosion, likely due to moderate rainfall and stabilized land use. The period between 2016 and 2023 reflects fluctuating but moderate erosion levels, suggesting a dynamic balance between erosive forces and conservation measures. This temporal trend emphasizes the need for year-specific conservation planning, especially during high-risk climatic periods.

Low risk, defined as soil loss ranging from 0 to 10 t ha⁻¹ yr⁻¹, covers approximately 95.5% of the basin, indicating effective ground cover and predominantly gentle terrain in most areas. Moderate risk, ranging from 10 to 20 t ha⁻¹ yr⁻¹, accounts for about 4.04% of the basin, primarily occurring in zones with moderately steep slopes or seasonal vegetation. Severe or high risk, exceeding 20 t ha⁻¹ yr⁻¹, occupies roughly

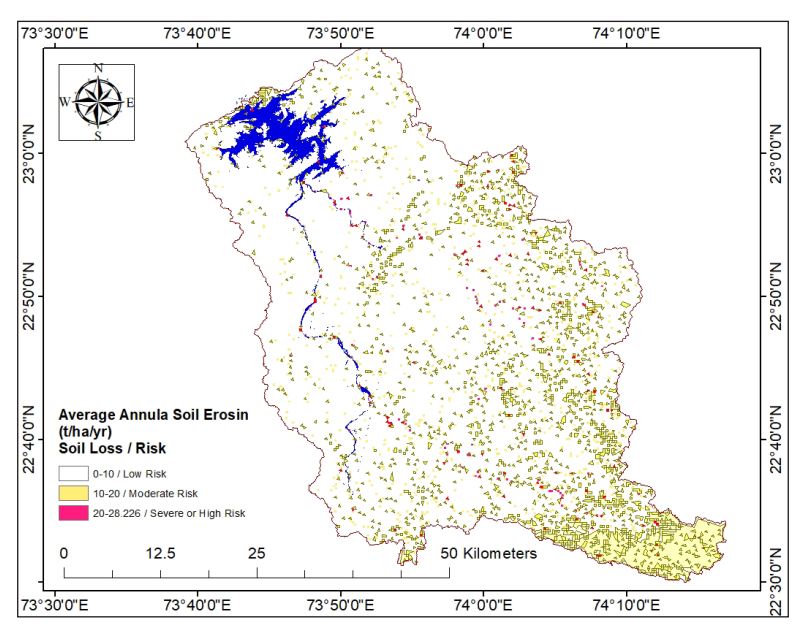


Fig. 5. Average annual soil erosion rate and risk zonation in Panam reservoir catchment

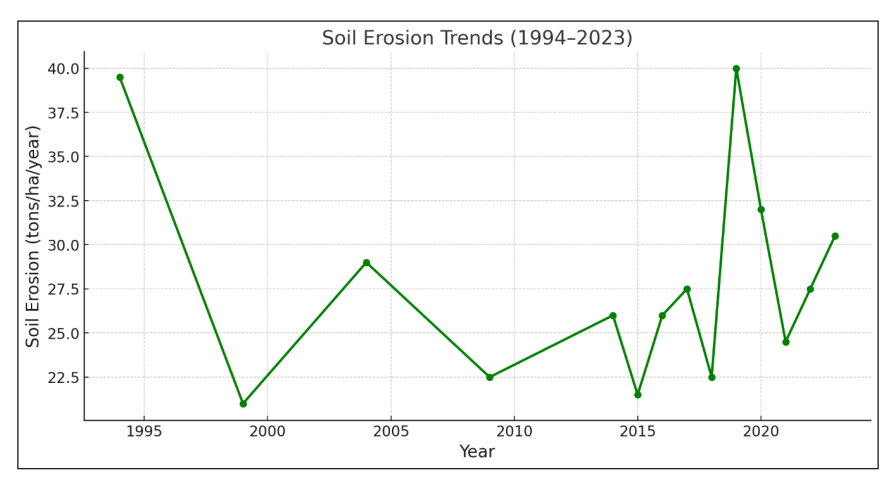


Fig. 6. Soil Erosion Trend in Panam Catchment (1994-2023).

Table 8. Soil loss categories and area coverage in the Panam catchment (based on the average annual soil loss rates derived from the RUSLE model)

Erosion Class	Soil Loss (t ha-1 yr-1)	Area (km²)	% of Basin
Low Risk	0-10	2256.36	95.50%
Moderate Risk	10-20	95.53	4.04%
Severe to High Risk	20-28.226	9.93	0.42%
Total	_	2361.82	100.00%

0.42% of the area and is typically associated with steep slopes, sparse vegetation, or bare land

Spatial Patterns of Erosion Drivers: The spatial analysis revealed distinct patterns in the distribution of erosion-related factors. Rainfall erosivity (R-factor) values were highest in the southwestern segments of the catchment, correlating with areas receiving intense monsoonal precipitation. The LSfactor, indicating topographic influence, was predominantly high in the hilly upstream regions, signifying steeper slopes and longer runoff paths. NDVI-based vegetation analysis indicated sparse cover in central and upper catchment zones, contributing to elevated C-factor values (0.409-0.437), which reflect poor surface protection. The P-factor analysis suggested minimal conservation with values clustered between 0.40 and 0.433, especially in steep, uncultivated lands. Together, these spatial drivers highlight erosion vulnerability hotspots that demand urgent conservation planning.

Model Validation: Validation of model outcomes was achieved by comparing RUSLE-derived soil loss estimates with empirical studies and observed trends in nearby watersheds such

as the Narmada and Rel River basins. Historical sediment deposition data and reservoir desiltation reports corroborated the spatial erosion patterns and magnitude observed in this study. The consistency of erosion hotspots, particularly in upper catchment zones, reinforces the robustness of the RUSLE-GIS integration in semi-arid monsoonal contexts. These comparative analyses affirm the model's credibility for regional planning applications.

Prioritization of Conservation Zones: To translate erosion risk analysis into actionable conservation planning, the catchment was subdivided into micro-watersheds using the watershed delineation tool in ArcGIS. A prioritization index (PI) was developed to rank these sub-watersheds based on three key parameters: severity of erosion (SE) - derived from RUSLE outputs; slope - extracted from the DEM and affected area (A) - proportion of each micro-watershed under high erosion risk

The index was computed as:

$$PI=(SE \times Slpe \times A\%)/1000$$
 ...9

Each micro-watershed was assigned a PI score and categorized into five priority classes: Very High, High, Moderate, Low, and Very Low. Zones with high slope and severe erosion

affecting a large area were classified as Very High Priority.

A Conservation Priority Map (Fig. 7) was generated to visualize spatial conservation targets across the catchment. This map reveals a clear spatial pattern in conservation urgency:

- The southern and central zones of the watershed are dominated by *Very High* and *High Priority* categories, characterized by high slope gradients, elevated RUSLE values, and substantial proportions of high-risk land.
- Conversely, the northern and northeastern regions primarily fall into *Low* and *Very Low Priority* categories, indicating stable geomorphology and reduced vulnerability.
- Approximately 21 micro-watersheds showed PI values of zero, suggesting either minimal erosion threat or negligible slope, and were excluded from immediate intervention planning.

This spatial prioritization is critical for guiding cost-effective soil and water conservation strategies such as afforestation, bunding, gully plugging, and check dam construction. It enables targeted intervention in erosion-prone areas, particularly in the upper catchment where degraded lands and sparse vegetation prevail. Furthermore, the methodology provides a replicable, scalable,

and data-driven framework for micro-watershed prioritization under national programs such as IWMP (Integrated Watershed Management Programme) and Soil Health Cards.

In conclusion, the conservation priority index map is not only a scientific output but a practical tool for integrated watershed development planning. By focusing interventions where they are needed most, this approach supports sustainable land management, enhances groundwater recharge, and mitigates sedimentation in downstream reservoirs.

Conclusion

This study has evolved a novel prioritization approach for erosion management based on a multi-criteria index combining slope, erosion severity, and spatial coverage of degraded areas. The prioritization map enables policymakers and watershed managers to identify subwatersheds with the highest urgency for intervention, improving resource targeting and efficiency. The method is adaptable to other basins and aligns with guidelines under IWMP and PMKSY programs in India. Based on the findings of this study, several actionable recommendations are proposed to mitigate soil erosion in the Panam catchment. These include initiating reforestation and establishing vegetative barriers on degraded upstream

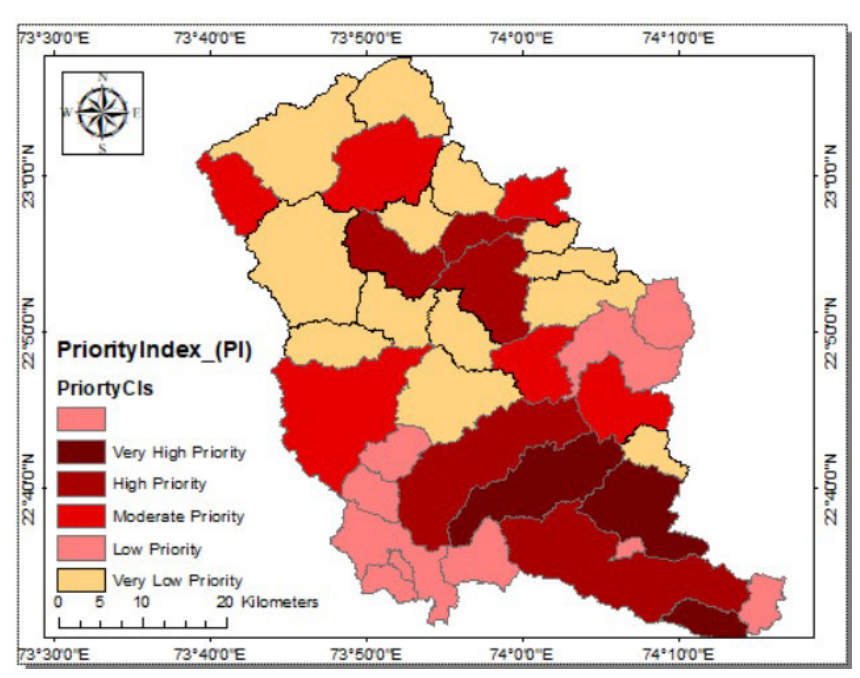


Fig. 7. Spatial Distribution of Soil Conservation Priorities in the Panam Watershed.

slopes to enhance root cohesion and reduce runoff velocity. Adoption of contour farming and terracing practices on undulating terrain can help interrupt slope length and promote infiltration. The construction of micro-check dams and gully plugs is essential for developing physical barriers in erosion gullies, aiding in sediment trapping and slope stabilization. Implementing soil health monitoring programs through annual assessments of topsoil nutrient status will enable early detection of degradation signs. Engaging stakeholders via community-based training and awareness campaigns will foster sustainable land use practices. Additionally, integrating RUSLEbased erosion risk maps into district-level watershed and disaster management plans can enhance strategic planning. Prioritizing microwatershed management efforts using indices that identify Very High Priority zones will ensure targeted and effective intervention.

References

- FAO Food and Agriculture Organization. (2003). Soil erosion assessment: Tools and guidelines for mapping and modeling soil erosion risk. Rome: FAO Land and Water Division.
- Ghosal, T. K. and Maiti, R. 2021. Estimation of rainfall erosivity index in Eastern India using empirical models. *Modeling Earth Systems and Environment* 7(2): 1121-1132. https://doi.org/10.1007/s40808-020-00969-4

- GSDMA (Gujarat State Disaster Management Authority) 2017. State Disaster Management Plan: Soil and Water Conservation Measures in Gujarat. Gandhinagar: Government of Gujarat.
- Moore, I.D. and Burch, G.J. 1986. Physical basis of the length-slope factor in the Universal Soil Loss Equation. *Soil Science Society of America Journal* 50(5): 1294-1298.
- Panagos, P., Borrelli, P., Meusburger, K., Alewell, C., Lugato, E. and Montanarella, L. 2015. Estimating the soil erosion cover-management factor at the European scale. *Land Use Policy* 48: 38-50. https://doi.org/10.1016/j.landusepol.2015.05.021
- Prasannakumar, V., Shiny, R.R., Geetha, N. and Vijith, H. 2012. Spatial prediction of soil erosion risk by remote sensing, GIS and RUSLE approach: A case study of Siruvani watershed, Western Ghats, India. *Environmental Earth Sciences* 64(4): 965-972. https://doi.org/10.1007/s12665-011-0901-3
- SCS (Soil Conservation Service) 2003. *National Engineering Handbook: Part 630 Hydrology.* United States Department of Agriculture (USDA), Washington, D.C.
- Van der Knijff, J.M., Jones, R.J.A. and Montanarella, L. 2000. *Soil erosion risk assessment in Europe*. European Soil Bureau.
- Wischmeier, W.H. and Smith, D.D. 1978. Predicting rainfall erosion losses: A guide to conservation planning (Agriculture Handbook No. 537). U.S. Department of Agriculture.

Printed in June 2025